Biosensors and Bioelectronics 129 (2019) 284–291

Contents lists available at ScienceDirect

Biosensors and Bioelectronics

journal homepage: www.elsevier.com/locate/bios

Electrochemiluminescence on smartphone with silica nanopores membrane modified electrodes for nitroaromatic explosives detection

Shuang Li[a,b], Danhua Zhang[a], Jinglong Liu[a], Chen Cheng[a], Long Zhu[b], Candong Li[b], Yanli Lu[a], Sze Shin Low[a], Bin Su[c], Qingjun Liu[a,b,*]

[a] Biosensor National Special Laboratory, Key Laboratory for Biomedical Engineering of Education Ministry, Department of Biomedical Engineering, Zhejiang University, Hangzhou 310027, PR China
[b] Collaborative Innovation Center of TCM Health Management, Fujian University of Traditional Chinese Medicine, Fuzhou 350108, PR China
[c] Institute of Microanalytical Systems, Department of Chemistry, Zhejiang University, Hangzhou 310058, PR China

ARTICLE INFO

Keywords:
Silica nanopores
Electrochemiluminescence
Smartphone
Polypeptides
Nitroaromatic explosives
Screen printed electrodes

ABSTRACT

Silica nanopores have electron channels and ion channels interpenetrating each other, which prompt the use of this structure for creating efficient electronic devices. In this study, silica nanopores membrane modified screen printed electrodes were applied in a smartphone-based electrochemiluminescence system for nitroaromatic explosives detection. Universal serial bus-on the go (USB-OTG) and camera on smartphone were used as the electrical stimulation and luminescence capture, respectively. □Multimode methods including (red-green-blue) RGB, (hue-saturation-brightness) HSB, and Gray were proposed for luminescence analysis. Specific polypeptides were immobilized on the nanopores modified electrodes for nitroaromatic explosives sensing. With positive-charged tris(2,2′-bipyridyl)ruthenium(II) ($Ru(bpy)_3^{2+}$) as electrochemiluminescence label, the increase in luminescence was associated with the selective ion channels and the well-conductive electron channels in the negative-charged nanopores. Besides, on account of the large specific surface area, nanopores modified screen printed electrodes showed stable and uniform luminescence. Results showed that the nanopores-enhanced electrochemiluminescence on smartphone covered a linear dynamic range from 10^{-7} mg/mL to 10^{-3} mg/mL for nitroaromatic explosives detection with the detection limit of 2.3×10^{-9} mg/mL. Therefore, high-efficient photo-electricity conversion capabilities of nanopores made it a kind of promising platform for sensitive and stable electrochemiluminescence. Furthermore, smartphone-based electrochemiluminescence with disposable screen printed electrodes could facilitate the mobile monitoring of biochemical analytes in the fields of environment, security, and health.

1. Introduction

Silica nanopores with the possession of pores from 2 nm to 50 nm, have aroused great attention in biochemical detection, due to their three-dimensional bicontinuous pore-ligament structures and high specific surface areas (Storm et al., 2005; de la Escosura-Muñiz and Merkoçi, 2011; Lin et al., 2015; Zugic et al., 2017). Their inherent lower toxicity, low production costs, and high degrees of ordering made nanopores be suitable as the solid support for sensitive layer. Besides, nanopores also possessed interpenetrating ionic paths and electronic paths, which led to efficient electrochemical performance (Poltorak et al., 2014; Huang et al., 2016). Especially, vertically oriented nanopores membrane on electrodes benefited the fast transportation in electroanalysis (Etienne et al., 2013; Walcarius, 2015). For instance, in electrochemiluminescence detection, nanopores exhibited fast charge transfer capability, low background current, and efficient photo-electricity conversion of luminophor materials (Wu et al., 2013; Zhai et al., 2015; Huo et al., 2017). As one of the most studied luminophors, tris (2,2′-bipyridyl)ruthenium(II) ($Ru(bpy)_3^{2+}$) with high stability and adaptability, could regenerate during electrochemiluminescence process without need to deliver extra reagent. This may result in simple and low-cost experimental design for electrochemiluminescence detection.

Electrochemiluminescence possesses several advantages, for example wide dynamic concentration response range, voltage controllability, high sensitivity and rapidity (Blackburn et al., 1991; Muzyka,

* Corresponding author at: Biosensor National Special Laboratory, Key Laboratory for Biomedical Engineering of Education Ministry, Department of Biomedical Engineering, Zhejiang University, Hangzhou 310027, PR China.
E-mail address: qjliu@zju.edu.cn (Q. Liu).

https://doi.org/10.1016/j.bios.2018.09.055
Received 1 July 2018; Received in revised form 14 September 2018; Accepted 14 September 2018
Available online 15 September 2018
0956-5663/

2014; Rizwan et al., 2018). On account of these excellent features, electrochemiluminescence has been established as an important detection technology for point of care testing. Traditional electrochemiluminescence is initiated by an electrochemical workstation and captured by a photomultiplier tube. The integration of electrochemiluminescence into "all-in-one device" is one attractive direction to design portable, user-friendly, and cost-effective detector for point of care testing (Delaney et al., 2013; Gao et al., 2017). Common-used smartphone, thanks to their open-source operation systems, high imaging, and computing capabilities, increasingly plays a pivotal role in electrochemical detection and optical detection (Vashist et al., 2014; Zhang and Liu, 2016; Xu et al., 2018; Bisetty, 2018). Therefore, electrochemiluminescence as the combination of electrochemistry and chemiluminescence, has the potential to realize on the phone for the development of portable devices on practical sensing application.

Trinitrotoluene and dinitrotoluene have gathered a lot of attention in explosives, whose release mainly caused by open detonation, poorly maintained ammunition disposal and storage (Toal and Trogler, 2006; Yang et al., 2010). Therefore, it is imperative to identify and investigate the possible pollution sites before the implementation of effective remediation steps. To selectively detect explosives, the electrode should be immobilized with molecular recognition component. Recently, short linear binding polypeptides obtained using phage display received extensive attention in nitroaromatic explosives sensing (Jaworski et al., 2008; Kuang et al., 2009; Hwang et al., 2011; Heller et al., 2011). Polypeptide is a short chain of amino acids with advantages, such as high stability and robustness to harsh environments, easily synthetic and immobilized method, cost and time efficiency (Cui et al., 2012; Pavan and Berti, 2012; Liu et al., 2015, 2016). The immobilization of polypeptides to various platforms has resulted in an upsurge in the development of functional polypeptides, also known as bifunctional polypeptides.

In this work, silica nanopores-enhanced electrochemiluminescence was developed on smartphone with universal serial bus-on the go (USB-OTG) as the electrical stimulation and camera to capture luminescence. A bifunctional polypeptide (Lys-Trp-His-Trp-Gln-Arg-Pro-Leu-Met-Pro-Val-Ser-Ile-Lys) was designed for nitroaromatic explosives detection. Lysine on the first and the end of the bifunctional polypeptide could be immobilized on silica nanopores modified screen printed electrodes by electrostatic adsorption. The middle of the bifunctional polypeptide could specifically bind with nitroaromatic explosives molecules. Positive-charged $Ru(bpy)_3^{2+}$ was applied as electrochemiluminescence label, whose luminescence signals were enhanced by the use of nanopores. Therefore, nanopores not only were the solid support for the immobilization of polypeptides, but also enhanced the electron transfer. So as to achieve signal amplification during electrochemiluminescence detection with a wide linear range, high sensitivity, and a low detection limit. Furthermore, lightweight, inexpensive, flexible, and disposable screen printed electrodes were applied in the smartphone based system, which was convenient to on-site biochemical detection.

2. Methods

2.1. Chemicals and materials

Cetyltrimethyl ammonium bromide (CTAB, $C_{19}H_{42}BrN$, MW: 364.45), tetraethoxysilane (TEOS, $C_8H_{20}O_4Si$, MW: 208.33), ammonium hydroxide (NH_4OH, MW: 35.05), hydrochloric acid (HCl, MW: 36.46), ethanol (C_2H_6O, MW: 46.07), acetone (C_3H_6O, MW: 58.08), potassium hydrogen phthalate (KHP, $C_8H_5KO_4$, MW: 204.22), potassium ferricyanide ($Fe(CN)_6^{3-}$, $K_3FeC_6N_6$, MW: 329.25), tris(2,2′-bipyridyl)ruthenium(II) hexahydrate ($Ru(bpy)_3^{2+}$, $C_{30}H_{24}Cl_2N_6Ru{\cdot}6H_2O$, MW: 748.62), tripropylamine (TPrA, $C_9H_{21}N$, MW: 143.27), 2,4,6-trinitrotoluene (TNT, $C_7H_5N_3O_6$, MW: 227.13), 2,4-dinitrotoluene (DNT , $C_7H_6N_2O_4$, MW: 182.13), 4-nitrotoluene (1NT, $C_7H_7NO_2$, MW: 137.14), trinitrophenol (TNP, $C_6H_3N_3O_7$, MW: 229.10), toluene (C_7H_8, MW: 92.14), nitrobenzoic acid ($C_7H_5NO_4$, MW: 167.13), benzylamine (C_7H_9N, MW: 108.16), methanol (CH_4O, MW: 32.04), and phosphate buffered saline (PBS, pH 7.4) were purchased from Sigma-Aldrich (USA). Screen printed electrodes (SPE) with carbon working electrode, carbon counter electrode and silver/silver chloride (Ag/AgCl) electrode were purchased from GSI Technologies (USA). The $Fe(CN)_6^{3-}$, $Ru(bpy)_3^{2+}$ and TPrA solutions are prepared with ultrapure water of 18.2 MΩ/cm. Methanol was used as the solvent of TNT, DNT, and 1NT.

2.2. Preparation of silica nanopores on electrodes

Before preparation of nanopores, the electrodes were thoroughly cleaned through ultrasonication for 30 min then washed in acetone, ethanol, and ultrapure water, successively. The preparation of silicon-based precursor fluids: cetyltrimethyl ammonium bromide (16 mg) was dissolved in 7 mL ultrapure water and stirred evenly. Then 3 mL ethanol was added to mixed solution and stirred to clarification. Tetraethoxysilane (8 μL) and ammonium hydroxide (1 μL) were added to the clarified liquid forming the precursor fluids. The cleaned electrodes were immersed in the precursor fluids and heated for 24 h in a water bath (60 °C). Then the electrodes were put in the oven at 100 °C for 24 h to get the cetyltrimethyl ammonium bromide closed membranes. In order to remove the template, the electrodes were put in 0.1 M hydrochloric acid and ethanol solution stirred for 30 min to get the nanopores modified electrodes.

2.3. Characterization of silica nanopores

The characterizations of the nanopores were performed on filed emission scanning electron microscope (SEM, Hitachi, SU8010), energy dispersive spectrum (EDS, Oxford-Inc., EMSA/MAS), transmission electron microscope (TEM, Hitachi, HT7700). SEM images showed the micromorphology of the blank electrodes, cetyltrimethyl ammonium bromide closed electrodes, and nanopores modified electrodes at the accelerating voltage of 3 kV. EDS images were applied to show the surface element distribution on the nanopores modified electrodes. For TEM sample preparation, nanopores membrane was scraped off the electrode surface by a knife and dispersed in ethanol. After 20 min ultrasonic processing, suspension liquid was put on the copper net for TEM imaging. Besides the characterization of microstructure, negative-charged $Fe(CN)_6^{3-}$ (50 mM) and positive-charged $Ru(bpy)_3^{2+}$ (50 mM) with potassium hydrogen phthalate (50 mM) as electrolyte were used to verified the electrification of the nanopores through cyclic voltammetry on an electrochemical workstation (PARSTAT 4000, AMETEK Inc., USA). The electrochemical detections were based on two-electrode system. The carbon working electrode on SPE was connected with working electrode connector in electrochemical workstation and carbon counter electrode connected together with Ag/AgCl electrode, acting as the other electrode of the system. Finally, differential scanning calorimetry (DSC, TA, Q200) was applied to study the melting behaviours of the nanopores modified electrode.

2.4. Polypeptides modified nanosensor

The polypeptide (Lys-Trp-His-Trp-Gln-Arg-Pro-Leu-Met-Pro-Val-Ser-Ile-Lys, MW: 1806.23) with the specific site of nitroaromatic explosives (Trp-His-Trp-Gln-Arg-Pro-Leu-Met-Pro-Val-Ser-Ile) was synthesized by solid phase method with stepwise addition of amino acids to a growing polypeptide chain. Two positive-charged lysine were added at the sides of the chain as the linking tail to the negative-charged nanopores. The property of the synthesized polypeptide was shown by high-performance liquid chromatography (HPLC) and mass spectrometry (MS). For

modification of the nanosenor, polypeptides were dissolved in PBS (pH 7.4) at the concentration of 100 μg/mL. The linkage of the polypeptides and nanosenor was through electrostatic adsorption. The polypeptides were distributed evenly on the nanopores modified electrodes for 24 h incubation. Then the electrodes were cleaned by PBS buffer to remove the unbonded polypeptides. Electrochemical impedance spectra were applied to characterize the polypeptides modified nanosensor on the electrochemical workstation. Cyclic voltammograms (scan rate: 50 mV/s) of the nanosensor in pH3, pH4, pH5, pH6, pH7, and pH8 were applied for the optimum pH. The nanosensor with polypeptides were stored under 4 ℃ and ready for nitroaromatic explosives detections.

2.5. Smartphone-based electrochemiluminescence system

Universal serial bus-On the go (USB-OTG) on the smartphone (HUAWEI G660-L075) was used as the electrical stimulation for luminescence. There are five lines in smartphone USB including GND, ID, D+, D-, and Vcc. Among them, D+ and D- were the data transfer ports, which were not used in our USB-OTG stimulated luminescence system. GND is electrical ground line as the potential reference. ID is used to identify the host device or slave device during USB-OTG communication. Vcc is the power line. Here, the carbon working electrode was linked with the Vcc port, carbon counter electrode and Ag/AgCl electrode were all linked with the GND port. ID pin connected electrically with the ground line, smartphone acted as the host device with a fixed 5 V voltage output. Through a divider circuit, the fixed voltage was divided into adjustable voltages from 2.0 V to 3.0 V for electrochemiluminescence. Luminescence images were captured by phone camera. Then the images were analyzed by self-compiled application (APP) software on the phone including red-green-blue (RGB), hue-saturation-brightness (HSB), and Gray analysis.

2.6. Nitroaromatic explosives detection

With 0.5 mM $Ru(bpy)_3^{2+}$ as luminophore and 50 mM TPrA as coreactant, the smartphone based electrochemiluminescence system was applied for nitroaromatic explosives detection. Trinitrotoluene, dinitrotoluene, and nitrotoluene standard solution were diluted to five different concentrations (10^{-7} mg/mL, 10^{-6} mg/mL, 10^{-5} mg/mL, 10^{-4} mg/mL, and 10^{-3} mg/mL). In order to illustrate the enhancement of nanopores on electrochemiluminescence, with and without nanopores modified sensors were used for nitroaromatic explosives detection. Cyclic voltammetry results from electrochemical workstation were used as the comparison with smartphone based system. The stability of the prepared electrode was measured continuously for 7 days with the concentration of 10^{-7} mg/mL. The selectivity was examined in the presence of the conventional contaminants, such as trinitrophenol, toluene, nitrobenzoic acid, and benzylamine with the concentration of 10^{-3} mg/mL. All of above detections were repeated for 5 times at room temperature (22 ℃).

3. Results and discussion

3.1. Electrochemiluminescence on smartphone

Considering the portability and real-time of detection, user-friendly smartphone was explored for electrochemiluminescence analysis (Fig. 1a). The source of motivation came from the USB-OTG on smartphone. The luminescence signals were captured by the rear camera on smartphone. In the electrochemiluminescence reaction system, $Ru(bpy)_3^{2+}$ was used as luminophore with TPrA as coreactant. The oxidative-reduction of $Ru(bpy)_3^{2+}$/TPrA occurred on the surface of the screen printed electrodes (Fig. 1b).

The reaction mechanism is as follows (Wei and Wang, 2011):

$$Ru(bpy)_3^{2+} - e^- \rightarrow Ru(bpy)_3^{3+} \quad (1)$$

$$TPrA - e^- \rightarrow TPrA^{+\cdot} \quad (2)$$

$$TPrA^{+\cdot} \rightarrow TPrA^{\cdot} + H^+ \quad (3)$$

$$Ru(bpy)_3^{3+} + TPrA^{\cdot} \rightarrow Ru(bpy)_3^{2+*} \quad (4)$$

$$Ru(bpy)_3^{2+*} \rightarrow Ru(bpy)_3^{2+} + h\nu \quad (5)$$

During the reaction, the $Ru(bpy)_3^{2+}$ luminophore was not consumed and could be recycled. This made the reaction system more economical. Besides, negative-charged nanopores were modified on the electrodes for enhanced $Ru(bpy)_3^{2+}$ luminescence. Specific polypeptides on the nanopores modified electrodes were applied in nitroaromatic explosives detection (Fig. 1c). Through built-in functional modules, our smartphone-based system integrated electric excitation, luminescence capture, and imaging analysis, which greatly promoted the user-friendliness of electrochemiluminescence detection. Moreover, inexpensive screen printed electrodes also improved the convenience of the detection, for that fibrous matrix did not impede diffusion and electrochemistry in paper appeared to work rather well. Therefore, smartphone-based electrochemiluminescence with disposable electrodes may facilitate the mobile monitoring of biochemical analytes.

3.2. Characterization of the silica nanopores

SEM images showed the microstructure of electrode surface, in which blank electrodes surface was very roughness (Fig. 2a), CTAB closed electrodes showed lots of large flat areas on the electrode surface (Fig. 2b), and nanopores modified electrodes showed uniformly distributed nanopores on the electrode surface (Fig. 2c). EDS analysis showed the element distribution on silica nanopores modified electrodes surface (Fig. 2d). The silica nanopores showed homogeneous distribution, in which silicon (Si) and Oxygenium (O) distributed widely and uniformly on the electrode surface. From the elements hierarchical mapping results (Fig. 2e), we could calculate the percentage of elements, such as Silicon (Si, 13.47%), Oxygenium (O, 45.06%), and Carbon (C, 41.47%).

In order to see the nanopores structure more clearly, we scraped the nanopores membrane off the electrode surface for TEM images. It could found that the area of nanopores film was about 1 μm^2 with smooth boundary (Fig. 2f). By local amplification, the details of the nanopores could be seen with the pore diameter about 2 nm (Fig. 2g). In Fig. S1, nanopores were full in the field of view, which could prove the good uniformity of the prepared nanopores. Sum up, nanopores showed good flatness, uniformity, and large specific surface area. These features may have benefit for electrochemical detection on the electrode surface. The melting peak of the screen printed electrodes was about 252.62 ℃. After the modification of nanopores, the melting peak of the electrode remained almost constant (Fig. S2). Therefore, the stable thermal effect of the original electrode was maintained by the nanopores.

3.3. Electrochemical properties of the nanosensor

Due to the deprotonation of silanol groups with an isoelectric point of 2–3, the nanopores are negatively charged (Etienne et al., 2007). Therefore, negative-charged $Fe(CN)_6^{3-}$ and positive-charged $Ru(bpy)_3^{2+}$ were used to characterize the electrochemical properties of the nanopores modified electrodes through cyclic voltammetry. CTAB closed membranes showed the worst conductivity. When the template was removed, nanopores modified electrodes showed repulsion to $Fe(CN)_6^{3-}$ (Fig. 3a) and attraction to $Ru(bpy)_3^{2+}$ (Fig. 3b). Usually, $Ru(bpy)_3^{2+}$ was the widely-used luminophors. Therefore, the nanopores would show the enhancement of effect in electrochemiluminescence signals. In Fig. S3, there almost were no responses from 0 V to 2 V.

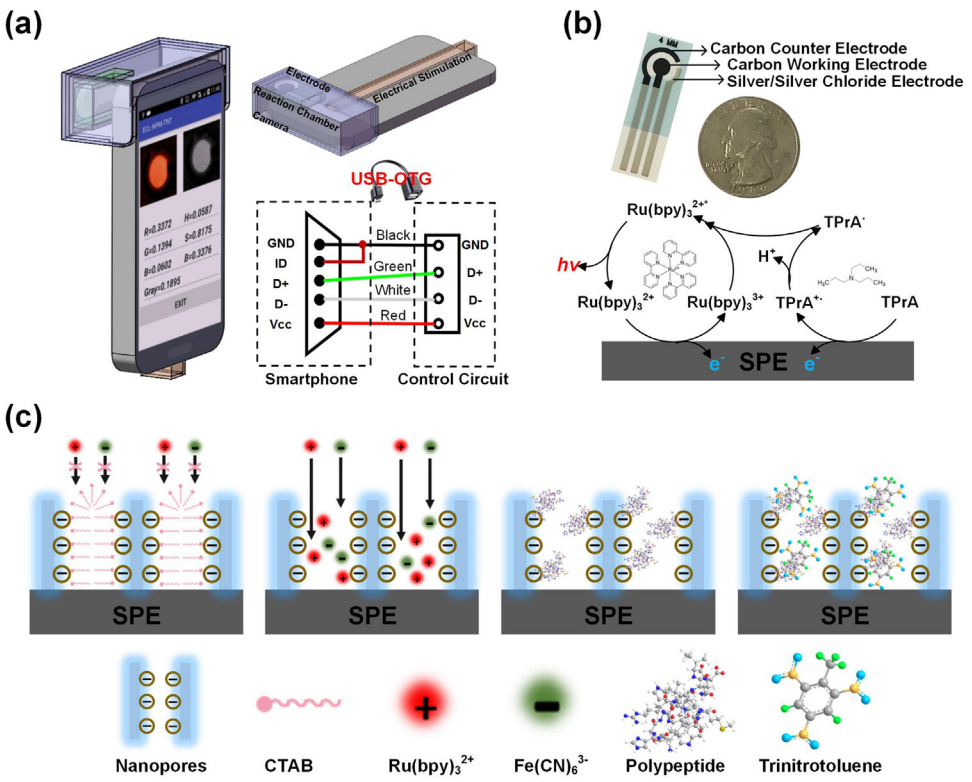

Fig. 1. Silica nanopores-enhanced electrochemiluminescence on smartphone. (a) Smartphone-based electrochemiluminescence system with reaction chamber and electrodes. USB-OTG was used as the electrical stimulation. Camera was used to capture luminescence images. (b) Top: pictures of screen printed electrodes (SPE) including carbon working electrode, carbon counter electrode, and Ag/AgCl electrode. During smartphone-based electrochemiluminescence detection, the carbon working electrode was linked with "Vcc" interface. The carbon counter electrode and Ag/AgCl electrode were all connected to "GND" interface. Bottom: reaction mechanism of $Ru(bpy)_3^{2+}$/TPrA luminescence assays on the electrodes. (c) Preparation of nanopores and immobilization of specific polypeptides on the electrodes for nitroaromatic explosives detection.

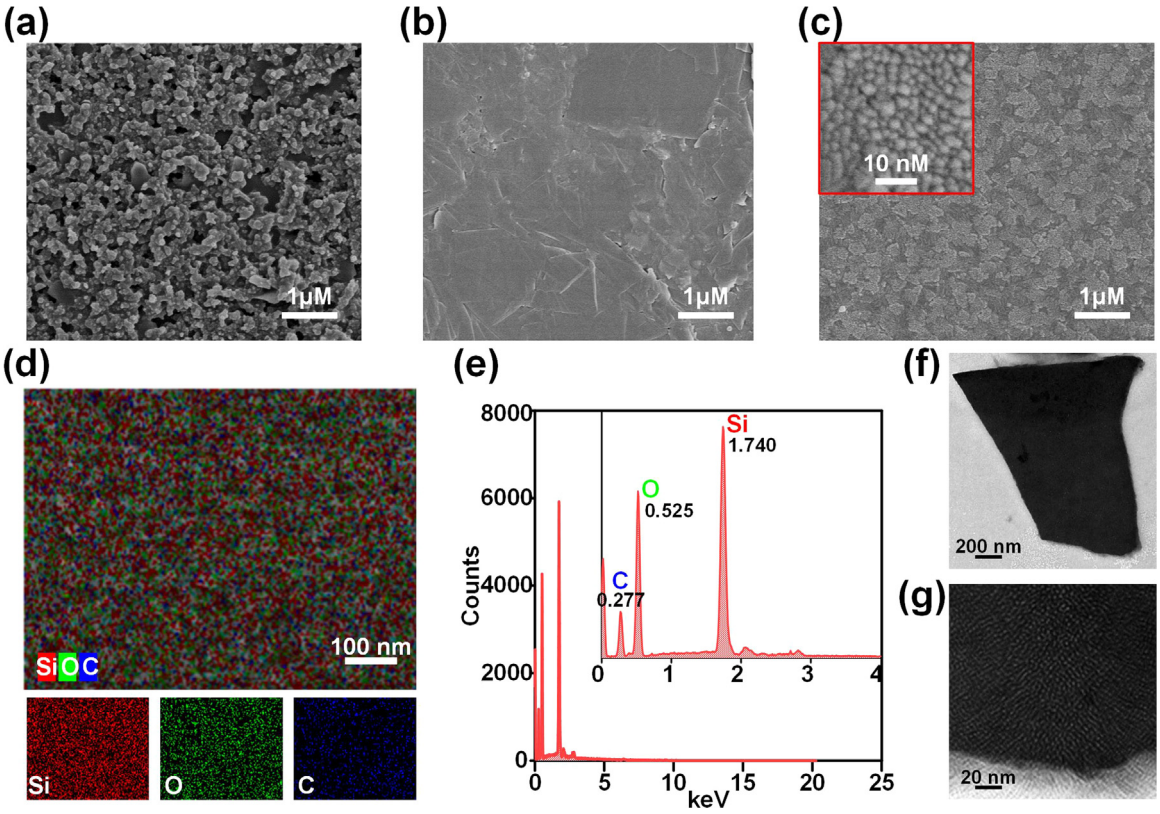

Fig. 2. Characterization of the silica nanopores. (a) SEM image of blank electrode under magnification of 10k. (b) SEM image of CTAB modified electrode under magnification of 10k. (c) SEM image of nanopores modified electrode under magnification of 10k (inset: partial enlarged SEM). (d) Elements hierarchical mapping of the nanopores modified electrode including Si (red), O (green), and C (blue). (e) EDS analysis of the nanopores modified electrode (inset: partial enlarged details). (f) TEM image of nanopores under magnification of 20k. (g) TEM image of nanopores under magnification of 200k.

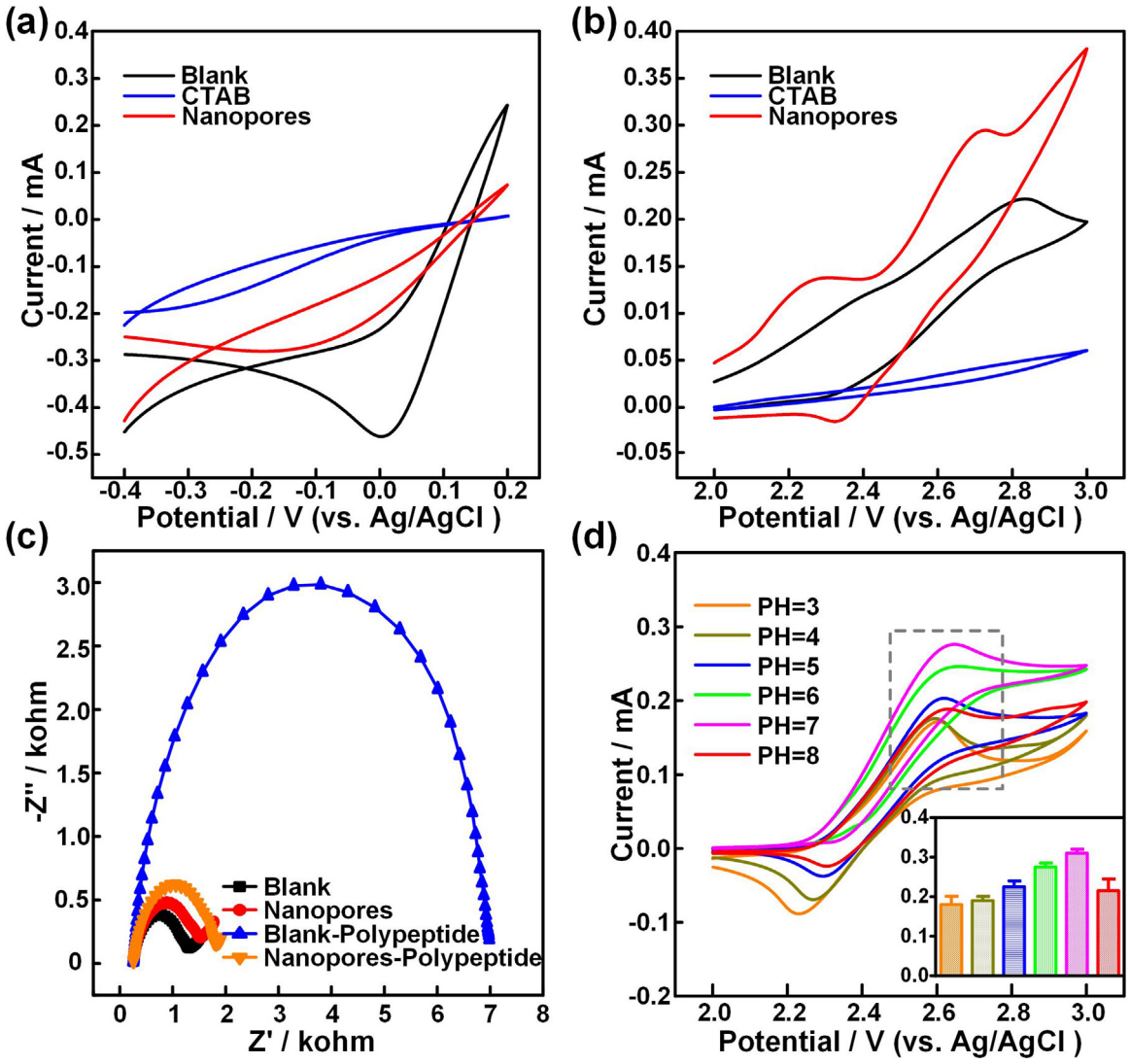

Fig. 3. Electrochemical properties of the nanosensor. (a) Cyclic voltammograms of the nanopores modified electrodes with scan rates of 50 mV/s in $Fe(CN)_6^{3-}$ from −0.4 to 0.2 V. (b) Cyclic voltammograms of the nanopores modified electrodes with scan rates of 50 mV/s in $Ru(bpy)_3^{2+}$ from 2.0 V to 3.0 V. (c) Electrochemical impedance spectra of the polypeptides modified nanosensor. (d) Cyclic voltammograms of the nanosensor in pH3, pH4, pH5, pH6, pH7, and pH8 (Inset: statistics results of peak current in different pH).

While the voltage reached 2.7 V, the current signal reached its maximum. Thus, the voltage range (2–3 V) was used to provide electrical excitation during electrochemiluminescence detection. In the electrochemical detection, as the Ag/AgCl electrode and carbon counter electrode were connected together, the Ag/AgCl electrode worked like a pseudo reference. In this two-electrode system, some of the voltage was consumed in the electrochemical cell, and thereby resulting in such a high voltage usage on the electrodes.

Specific polypeptides were modified on the nanopores for nitroaromatic explosives detection. The polypeptides were synthesized by solid phase method, whose property was shown by HPLC (Table S1). The chromatogram (Fig. S4) and chromatography analysis (Table S2) showed that the highest response appeared at Peak 3 (9.417) with the concentration proportion of 96.2469%. This illustrated that the synthetic polypeptides had high purity. Besides, mass spectrum further proved the polypeptides-14 (Lys-Trp-His-Trp-Gln-Arg-Pro-Leu-Met-Pro-Val-Ser-Ile-Lys, MW: 1806.23) from atomic mass point of view (Fig. S5).

After, two methods were used for the immobilization of polypeptides on the electrode. One was physical absorption, in which polypeptides were directly added and dried on the electrode surface. The other was electrostatic adsorption, in which positive-charged polypeptides were modified on the electrodes through negative-charged nanopores. Results showed that polypeptides directly modified electrode possessed high impedance, while polypeptides modified by nanopores showed little impedance changes than blank electrode (Fig. 3c). On account of the weak inductive of biochemical membranes, physical absorption without pertinence could largely induced the ability of electron transfer on electrode, which was adverse to electrochemical detections. In comparison, nanopores-based electrostatic adsorption not only had pertinence to target molecules, but also could make the target molecules with neat arrangement. Fig. 3d showed that with the progressive increment of pH values, the electrochemiluminescence currents increased. However, when the pH value reached 8, current signal decreased with voltammogram variation. Therefore, the optimum pH was 7 for the biosensor.

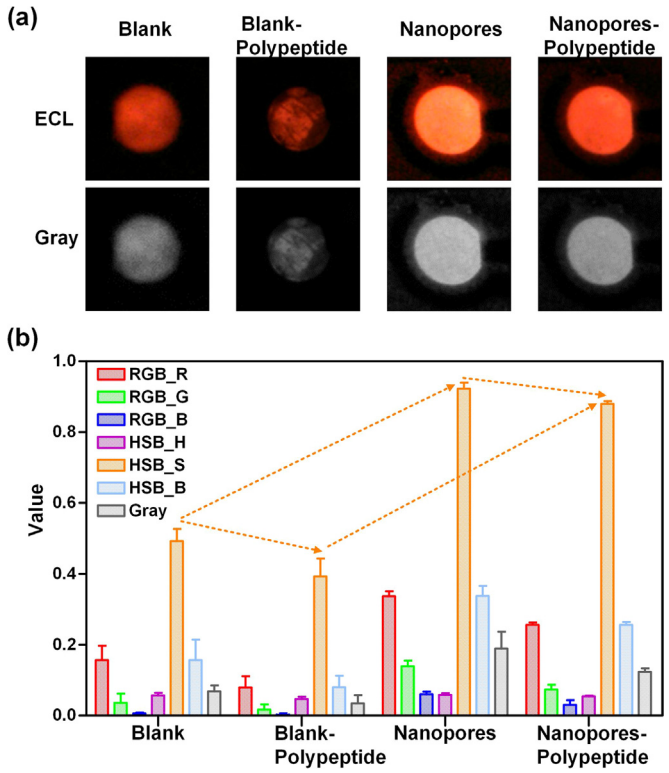

Fig. 4. Multimode luminescence analysis on smartphone. (a) ECL images and Gray images of the polypeptides modified nanosensor. (b) RGB, HSB, and Gray analysis of the luminescence images.

3.4. Multi-mode luminescence analysis on smartphone

Besides the characterization of electrochemical impedance spectroscopy, polypeptides modified nanosensor was also characterized by electrochemiluminescence on smartphone. Electrochemiluminescence images and Gray images showed that nanopores modified sensor possessed the enhancement to luminescence. After the immobilization of polypeptides on the nanosensor, nanopores modified sensor showed homogeneous and enhanced luminescence signals comparing with blank sensor (Fig. 4a). Further, multimode methods including RGB, HSB, and Gray were proposed to give specific data for luminescence analysis (Fig. 4b). All results of RGB_R, RGB_G, RGB_B, HSB_H, HSB_S, HSB_B, and Gray parameters showed the enhancement of nanopores in electrochemiluminescence and the decrease of luminescence after polypeptide modification. Even nanopores with polypeptides also possessed higher signals than blank sensor. Electrochemical workstation results also validated the nanopores' effect during electrochemiluminescence (Fig. S6), in which the change trend of current signals was in accordance with multimode color analysis. All results evidenced the advantages of nanopores-based sensor in the immobilization of biochemical membranes and electrochemiluminescence detections.

Among multimode methods, RGB and HSB were used to analyze the original luminescence images, Gray was used to analyze grayscale images. RGB is a widely-used and device-dependent model, which could be convert to HSB and Gray methods through specific calculation. While, perceptual and psychological non-intuitivism of human generated the problems with the visualization of R, G and B attributes. Such shortcomings could be overcame by utilizing hue, saturation, and brightness since HSB color model was the natural way for humans of describing colors. In our study, HSB_S had the highest response signal in multimode color methods, which was benefit for follow biochemical analysis.

3.5. Nitroaromatic explosives detection

Nitroaromatic compounds are found to be an important environmental, security, and health concern for the global community, because they are used as precursors for the manufacture of explosives in industry and military activities (Psillakis and Kalogerakis, 2001; Sohn et al., 2003; Gole et al., 2011). Methods for explosives detection included fluorescence (Germain and Knapp, 2009), surface enhanced Raman spectroscopy (Dasary et al., 2009), gas chromatography-mass spectrometer (Berg et al., 2007), and energy-dispersive X-ray diffraction (Luggar et al., 1998). Though these techniques showed high sensitivity and selectivity, some equipment was expensive and others could not be field in a portable, low-power package. However, high portability of the electrochemical instrumentation can be incorporated into inexpensive and portable devices for distinguishing and detecting nitroaromatic explosives (Hrapovic et al., 2006; Zhang et al., 2015; Shahdost-fard and Roushani, 2017; Tan et al., 2017). Usually, nitroaromatic explosives owned strong electron-withdrawing property, who were widely applied in electrochemical detections.

Here, smartphone-based electrochemiluminescence with nanopores and polypeptides were used for nitroaromatic explosives detection. As shown in Fig. 5a, with the increase of concentration, electrochemiluminescence images and Gray images grew progressively darker. RGB, HSB and Gray analysis showed the linear concentration changes from 10^{-7} mg/mL to 10^{-3} mg/mL, in which HSB_S possessed the highest strength (Fig. 5b). Besides, results from electrochemical workstation proved the decrease of currents with increasing concentrations (Fig. S7), which further verified the results from smartphone.

As a contrast, sensors without nanopores were also used for nitroaromatic explosives detection. Electrochemiluminescence images and Gray images showed heterogeneous luminescence signals (Fig. S8), which was on account of the uneven polypeptides modification without nanopores. RGB, HSB and Gray analysis showed small values than nanopores-based sensor, HSB_S was also the highest with good linearity (Fig. S9). Similarly, the current signals decreased with the concentrations of nitroaromatic explosives detection (Fig. S10). The comparison in current analysis showed that the slope of nanopores-based sensor was about twice over that without nanopores (Fig. S11). The comparison in luminescence images were implemented in RGB, HSB, and Gray models, respectively. In RGB analysis, RGB_R had the highest response, in which the slope of nanopores-based sensor was about twice over that without nanopores (Fig. 5c). The comparison results of RGB_G and RGB_B parameters also show the signal increase with nanopores (Figs. S12–13). In HSB analysis, HSB_S with the highest response, showed the slope increased from −0.0433 to −0.1300 (Fig. 5d). The comparison results of HSB_H and HSB_B parameters were shown in Figs. S14–15, which was in accordance with overall trend. Finally, analysis of the gray images also prove the enhancement of nanopores in electrochemiluminescence during biochemical detection (Fig. 5e). As a whole, nanopores-based electrochemiluminescence showed stable and enhanced luminous signals. Results of above could be discovered that HSB_S was the most principal parameters in luminescence images. Based on these results, the detection limit of trinitrotoluene from HSB_S analysis was 2.3×10^{-9} mg/mL. Besides, a week of continuous testing showed that the prepared electrode had good stability (Fig. S16). Even in the partial enlargement images, the overall fluctuation was within the range of the first day's measurement.

3.6. Specific detection

Trinitrotoluene, dinitrotoluene, and nitrotoluene showed luminescence quenching phenomenon, in which HSB_S changes increased with the increase of concentrations. Among them, trinitrotoluene showed the strongest ability to absorb electrons (Fig. 6a-b). Methanol as the blank control, almost had no changes to luminescence. Linear fitting results showed that the polypeptide modified nanosensor had high selectivity

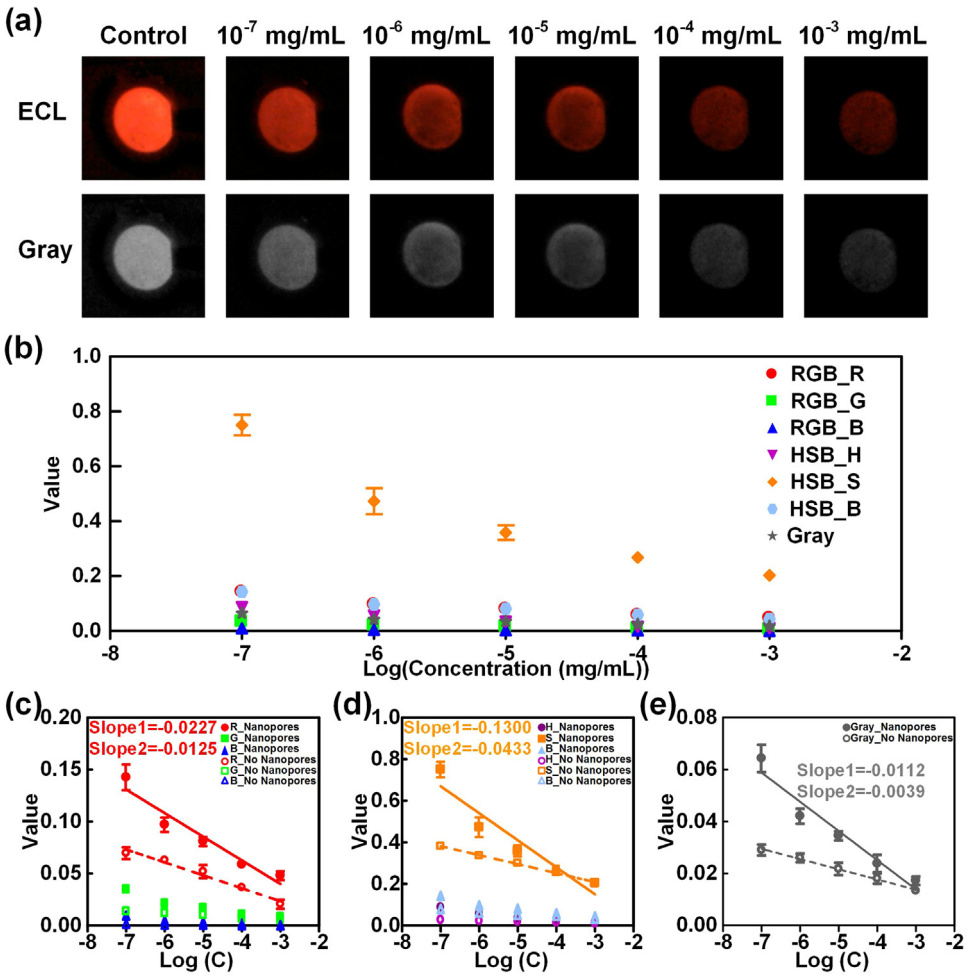

Fig. 5. Nanosensor with nanopores and polypeptides for nitroaromatic explosives detection on smartphone. (a) ECL images and Gray images of the detection from 10^{-7} mg/mL to 10^{-3} mg/mL. (b) RGB, HSB, and Gray analysis of the detection on the nanopores modified electrodes. (c) Comparison of the detection with nanopores and without nanopores in RGB analysis. (d) Comparison of the detection with nanopores and without nanopores in HSB analysis. (e) Comparison of the detection with nanopores and without nanopores in Gray analysis. (All detections were repeated for 5 times.).

to nitroaromatic explosives, especially trinitrotoluene (Fig. 6c-d). Besides, agree with the previous results, nanopores played the role of magnifying signals, which increased the detection sensitivity of the system. For selectivity tests, we have examined the conventional interferents, such as trinitrophenol, toluene, nitrobenzoic acid, benzylamine with the concentration of 10^{-3} mg/mL. Fig. S17 showed that our polypeptide modified sensor had good selectivity towards trinitrotoluene. Trinitrophenol called picric acid, was also a kind of explosives. For trinitrophenol has the similar structure with trinitrotoluene, the mixed test of trinitrotoluene and trinitrophenol was further applied for the verification of selectivity. Results showed that our sensor also had good selectivity even in the mixed test.

Selectivity and sensitivity are the main challenges in the design of a biosensor platform. Selectivity can be achieved by using biological recognition elements. Biomimetic sensing usually needs to adapt the biological principles, select sensitive materials, and process signals. Recently, using polypeptides as discerning element has been particularly advantageous for there have been several mature synthesis protocols to tailor polypeptide structures. Besides, polypeptides could be modified to be stable under many different environments, which greatly broadened their application scenarios. Through the development of bifunctional peptides, which could also bind onto desired sensors. Therefore, bifunctional polypeptides would be a kind of optional strategy for biosensor design to address the need and challenge for selective, sensitive, and accurate detection in biochemical identification and quantification. As for sensitivity, we designed nanopores-enhanced electrochemiluminescence. Results illustrated that nanopores had permselective ion channels, which would benefit the transfer of Ru $(bpy)_3^{2+}$ luminophors at the electrode surface. Furthermore, uniform arrangement of nanopores was conducive to recognition elements modification, which would also increase the sensitivity of the detection.

4. Conclusion

In this work, a smartphone-based electrochemiluminescence system for rapid and sensitive detection of nitroaromatic explosives was accomplished on silica nanopores membrane modified electrodes. In the system, universal serial bus-on the go (USB-OTG) provided the stable electrical stimulation. Then phone camera captured the luminescence images, which were further analyzed by RGB, HSB, and Gray. The multimode methods provided comprehensive analysis with the detection limit of 2.3×10^{-9} mg/mL. Nanopores-enhanced electrochemiluminescence showed excellent performance in biochemical sensing with acceptable reproducibility, stability, sensitivity, and convenient operability. With the modification of specific recognition polypeptides, the sensor also showed high selectivity towards nitroaromatic explosives detection. Therefore, the combination of smartphone-based system with biosensor would greatly promote the development of mobile monitoring in biochemical analysis.

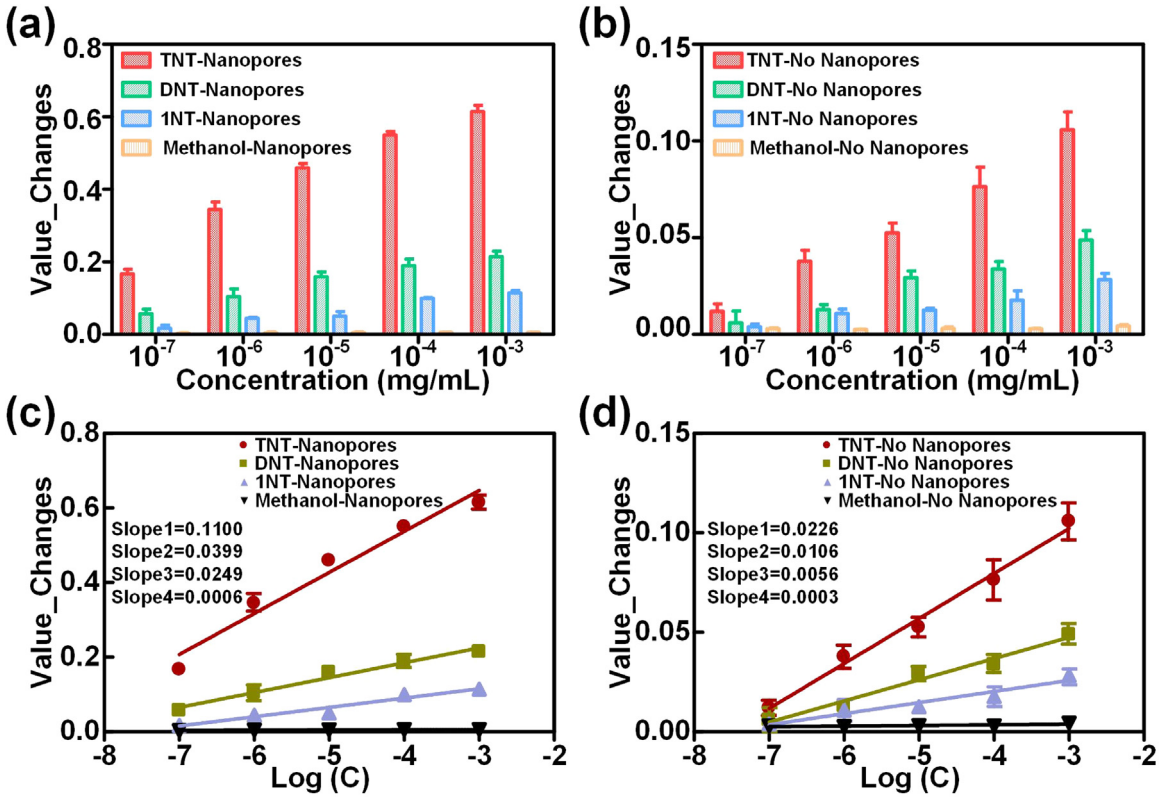

Fig. 6. TNT, DTN, 1NT, and methanol detection on the smartphone-based ECL system. (a) Value changes of the detection in HSB_S analysis with nanopores. (b) Values changes of the detection in HSB_S analysis without nanopores. (c) Linear fitting curve of the detection in HSB_S analysis with nanopores. (d) Linear fitting curve of the detection in HSB_S analysis without nanopores.

Acknowledgment

This work was supported by the National Natural Science Foundation of China (Grant no. 31671007), the Zhejiang Provincial Natural Science Foundation of China (Grant No. LZ18C100001)), the China Postdoctoral Science Foundation (Grant No. 2018M630677), and the Collaborative Innovation Center of Traditional Chinese Medicine Health Management of Fujian Province of China.

Appendix A. Supporting information

Supplementary data associated with this article can be found in the online version at doi:10.1016/j.bios.2018.09.055.

References

Berg, M., Bolotin, J., Hofstetter, T.B., 2007. Anal. Chem. 79, 2386–2393.
Bisetty, K., 2018. Biosens. Bioelectron. 102, 136–149.
Blackburn, G.F., Shah, H.P., Kenten, J.H., Leland, J., Kamin, R.A., Link, J., Peterman, J., Powell, M.J., Shah, A., Talley, D.B., 1991. Clin. Chem. 37, 1534–1539.
Cui, Y., Kim, S.N., Naik, R.R., McAlpine, M.C., 2012. Acc. Chem. Res. 45, 696–704.
Dasary, S.S., Singh, A.K., Senapati, D., Yu, H., Ray, P.C., 2009. J. Am. Chem. Soc. 131, 13806–13812.
Delaney, J.L., Doeven, E.H., Harsant, A.J., Hogan, C.F., 2013. Anal. Chim. Acta 803, 123–127.
de la Escosura-Muñiz, A., Merkoçi, A., 2011. Small 7, 675–682.
Etienne, M., Quach, A., Grosso, D., Nicole, L., Sanchez, C., Walcarius, A., 2007. Chem. Mater. 19, 844–856.
Etienne, M., Guillemin, Y., Grosso, D., Walcarius, A., 2013. Anal. Bioanal. Chem. 405, 1497–1512.
Gao, W., Saqib, M., Qi, L., Zhang, W., Xu, G., 2017. Curr. Opin. Electrochem.
Germain, M.E., Knapp, M.J., 2009. Chem. Soc. Rev. 38, 2543–2555.
Gole, B., Bar, A.K., Mukherjee, P.S., 2011. Chem. Commun. 47, 12137–12139.
Heller, D.A., Pratt, G.W., Zhang, J., Nair, N., Hansborough, A.J., Boghossian, A.A., Reuel, N.F., Barone, P.W., Strano, M.S., 2011. Proceedings of the National Academy of Sciences 108, pp. 8544–8549.
Hrapovic, S., Majid, E., Liu, Y., Male, K., Luong, J.H., 2006. Anal. Chem. 78, 5504–5512.
Huang, X., Xie, L., Lin, X., Su, B., 2016. Anal. Chem. 88, 6563–6569.
Huo, X.-L., Yang, H., Zhao, W., Xu, J.-J., Chen, H.-Y., 2017. ACS Appl. Mater. Interfaces 9, 33360–33367.
Hwang, K.S., Lee, M.H., Lee, J., Yeo, W.-S., Lee, J.H., Kim, K.-M., Kang, J.Y., Kim, T.S., 2011. Biosens. Bioelectron. 30, 249–254.
Jaworski, J.W., Raorane, D., Huh, J.H., Majumdar, A., Lee, S.-W., 2008. Langmuir 24, 4938–4943.
Kuang, Z., Kim, S.N., Crookes-Goodson, W.J., Farmer, B.L., Naik, R.R., 2009. ACS nano 4, 452–458.
Lin, X., Yang, Q., Ding, L., Su, B., 2015. ACS nano 9, 11266–11277.
Liu, Q., Wang, J., Boyd, B.J., 2015. Talanta 136, 114–127.
Liu, X., Marrakchi, M., Xu, D., Dong, H., Andreescu, S., 2016. Biosens. Bioelectron. 80, 9–16.
Luggar, R., Farquharson, M., Horrocks, J., Lacey, R., 1998. X-Ray Spectrom.: Int. J. 27, 87–94.
Muzyka, K., 2014. Biosens. Bioelectron. 54, 393–407.
Pavan, S., Berti, F., 2012. Anal. Bioanal. Chem. 402, 3055–3070.
Poltorak, L., Herzog, Gg, Walcarius, A., 2014. Langmuir 30, 11453–11463.
Psillakis, E., Kalogerakis, N., 2001. J. Chromatogr. A 907, 211–219.
Rizwan, M., Mohd-Naim, N.F., Ahmed, M.U., 2018. Sensors 18, 166.
Shahdost-fard, F., Roushani, M., 2017. Biosens. Bioelectron. 87, 724–731.
Sohn, H., Sailor, M.J., Magde, D., Trogler, W.C., 2003. J. Am. Chem. Soc. 125, 3821–3830.
Storm, A.J., Storm, C., Chen, J., Zandbergen, H., Joanny, J.-F., Dekker, C., 2005. Nano Lett. 5, 1193–1197.
Tan, C., Nasir, M.Z.M., Ambrosi, A., Pumera, M., 2017. Anal. Chem. 89, 8995–9001.
Toal, S.J., Trogler, W.C., 2006. J. Mater. Chem. 16, 2871–2883.
Vashist, S.K., Mudanyali, O., Schneider, E.M., Zengerle, R., Ozcan, A., 2014. Anal. Bioanal. Chem. 406, 3263–3277.
Walcarius, A., 2015. Electroanalysis 27, 1303–1340.
Wei, H., Wang, E., 2011. Luminescence 26, 77–85.
Wu, L., Li, M., Zhang, M., Yan, M., Ge, S., Yu, J., 2013. Sens. Actuators B: Chem. 186, 761–767.
Xu, D., Huang, X., Guo, J., Ma, X., 2018. Biosens. Bioelectron.
Yang, J., Aschemeyer, S., Martinez, H.P., Trogler, W.C., 2010. Chem. Commun. 46, 6804–6806.
Zhai, Q., Zhang, X., Han, Y., Zhai, J., Li, J., Wang, E., 2015. Anal. Chem. 88, 945–951.
Zhang, D., Liu, Q., 2016. Biosens. Bioelectron. 75, 273–284.
Zhang, D., Jiang, J., Chen, J., Zhang, Q., Lu, Y., Yao, Y., Li, S., Liu, G.L., Liu, Q., 2015. Biosens. Bioelectron. 70, 81–88.
Zugic, B., Wang, L., Heine, C., Zakharov, D.N., Lechner, B.A., Stach, E.A., Biener, J., Salmeron, M., Madix, R.J., Friend, C.M., 2017. Nat. Mater. 16, 558.